Journal of the Earth and Space Physics
Homepage: https://jesphys.ut.ac.ir
Vol. 51, No. 4, Winter 2026, P. 13-27
(Research Article)

Global-Scale Numerical Modeling of Seismic Wave Propagation Using PREM and Unstructured Triangular Meshing: Insights into the Layered Structure of Earth

Yazdanpanah, A.[1] | Abedi, M.[1] ✉

1. School of Mining Engineering, College of Engineering, University of Tehran, Tehran, Iran.

Corresponding Author E-mail: maysamabedi@ut.ac.ir

(Received: 13 July 2025, Revised: 9 Dec 2025, Accepted: 3 Feb 2026, Published online: 17 March 2026)

Abstract

The Preliminary Reference Earth Model (PREM) provides a robust framework for understanding seismic wave propagation through Earth's layered interior. This study employs numerical forward modeling to simulate P-wave and S-wave ray paths, travel times, and apparent velocity curves within a 2D unstructured triangular mesh based on PREM. The mesh was optimized for numerical stability, achieving a mean element quality of 0.91 and facilitating accurate interpolation of PREM's velocity profiles. Seismic responses are compared with those from simplified homogeneous and linear gradient velocity models to highlight the influence of Earth's layered structure. Validation against an analytical homogeneous benchmark yielded a mean travel-time relative error of only ~0.3%, while comparative analysis revealed that the linear gradient model deviates from PREM by as much as ~32% at the core-mantle boundary. Results demonstrate that PREM's velocity heterogeneities and discontinuities, such as the core-mantle boundary and liquid outer core, produce complex ray paths and variable apparent velocities, contrasting the straight paths and uniform velocities of the homogeneous model and the smoother trends of the gradient model. These findings underscore the necessity of detailed velocity models and advanced unstructured discretization for realistic seismic simulations. By providing a reproducible computational framework, this study affirms the effectiveness of advanced numerical techniques in capturing Earth's internal dynamics. It emphasizes the critical role of layering in seismic wave behavior, offering insights into the development of next-generation Earth models.

Keywords: Wave Propagation, Preliminary Reference Earth Model (PREM), Forward Modeling, Velocity, Ray-Tracing.

1. Introduction

The Preliminary Reference Earth Model (PREM), introduced by Dziewonski and Anderson in 1981 (Dziewonski & Anderson, 1981), has served as the foundational one-dimensional (1D) model for Earth's seismic velocities for decades. PREM was meticulously constructed by integrating diverse geophysical datasets, including free oscillation measurements, surface wave dispersion, body-wave travel times, and astronomical observations. This comprehensive model provides detailed profiles of P-wave and S-wave velocities, density, and attenuation, all characterized as functions of depth. Notably, PREM incorporates transverse isotropy within the upper mantle, a crucial feature designed to accurately fit observed Love and Rayleigh wave dispersion data (Bormann et al., 2012; Shearer, 2009).

While PREM remains a cornerstone, with most contemporary Earth models exhibiting values close to its parameters, notable discrepancies persist. The most significant differences are often observed in the upper mantle, particularly concerning the enigmatic 220 km discontinuity (Shearer, 2009). Given the substantial advancements in seismology and related geosciences since PREM's inception, there is a continuous scientific discourse advocating for the development of a next-generation reference Earth model.

Considerable effort has been dedicated to refining and developing alternative 1D Earth models since the publication of PREM, driven by the increasing volume and precision of seismic data. For instance, new spherically symmetric P- and S-wave

Cite this article: Yazdanpanah, A., & Abedi, M., (2026). Global-Scale Numerical Modeling of Seismic Wave Propagation Using PREM and Unstructured Triangular Meshing: Insights into the Layered Structure of Earth. *Journal of the Earth and Space Physics*, 51(4), 13-27. DOI: http//doi.org/10.22059/jesphys.2026.397888.1007701

E-mail: (1) amiryazdanpanah2@gmail.com

Publisher: University of Tehran Press.
DOI: http//doi.org/10.22059/jesphys.2026.397888.1007701
Print ISSN: 2538-371X
Online ISSN: 2538-3906

velocity models have been rigorously proposed, exhibiting notable variations from PREM, particularly within the complex lower mantle and outer core regions, where seismic wave behavior is critical for understanding Earth's deep interior (Morelli & Dziewonski, 1993; Song & Helmberger, 1995). Furthermore, sophisticated attempts have been made to systematically reconcile disparities between reference models derived from disparate data types, such as body-wave travel times and normal-mode observations. This has often been achieved through the incorporation of more refined anelasticity and anisotropy parameters, leading to models that offer a more cohesive global picture of Earth's elastic and anelastic structure (Montagner & Kennett, 1996).

Beyond purely seismic constraints, the compatibility of large-scale mantle convection hypotheses with seismic data has been thoroughly tested. This interdisciplinary approach has led to the development of physical reference models for the upper mantle and transition zone that effectively integrate both seismic observations and constraints from mineral physics, providing a more geo-dynamically consistent view of Earth's composition and thermal state (Cammarano et al., 2005).

More recently, innovative methodologies have emerged, including novel approaches involving the global coda-correlation wavefield. This new paradigm in global seismology has facilitated the derivation of entirely new reference Earth models, which display radial seismic velocity differences compared to established models, especially near first-order discontinuities like the core-mantle and inner-core boundaries, offering independent constraints on Earth's deep structure (Ma & Tkalčić, 2021).

The broad utility of PREM's fundamental parameters, including its density profiles along with those from other models like AK135-F, has been further assessed. These assessments affirm their suitability for defining robust 1D reference density models, proving invaluable for validating numerical methods in global and large-scale gravimetric forward and inverse modeling (Tenzer et al., 2022). Its applicability extends beyond core seismological studies into broader geoscientific and even planetary science domains, where it has been leveraged as a foundational basis for deriving semi-empirical mass-radius relations for rocky exoplanets (Zeng et al., 2016).This model also plays a crucial role in computing essential geodetic parameters such as load Love numbers and Green's functions, critical in studies related to Earth's deformational responses to surface loading processes (Wang et al., 2012).

Despite its widespread and enduring influence, scholarly discussions regarding the mechanical consistency of certain aspects of PREM, such as the isotropic ball approximation applied to the inner core, continue to be actively explored from a nonlinear geomechanics perspective, indicating ongoing efforts to refine its physical interpretations (Guliyev & Javanshir, 2020). Further comprehensive details on Earth's intricate internal structure and the principles governing seismic wave propagation can be found in authoritative texts (Ammon et al., 2021).

Numerical methods have become indispensable in seismic analysis and modeling, enabling sophisticated simulations of wave propagation and structural responses. The Finite Element Method (FEM), for instance, has found extensive application in diverse contexts, with recent advancements leading to high-order accuracy versions that significantly improve performance and precision in seismic modeling (De Basabe & Sen, 2009). Complementing these developments, unconventional model discretization techniques such as unstructured triangular meshing offer substantial benefits for complex seismic simulations. They enable the accurate representation of intricate geometries and highly heterogeneous velocity fields, which are crucial for realistic Earth models. This approach facilitates large-scale simulations, including coupling between fluid and solid regions and the incorporation of detailed topographical or geological features, often with reduced memory requirements compared to traditional grid-based methods (Peter et al., 2011; Rettenberger & Bader, 2015; Rüger & Hale, 2006). Collectively, these advancements in FEM and unstructured meshing have profoundly enhanced the capabilities for modeling seismic wave propagation and for conducting seismic

inversion studies.

In this study, we implement a 2D representation of the fundamentally 1D radial PREM. We maintain assumptions of spherical symmetry and the absence of lateral heterogeneity to specifically isolate the influence of radial stratification on seismic observables. The primary novelty of this work lies in the high-fidelity integration of P-wave, S-wave, and density profiles of PREM into a high-quality unstructured mesh framework. Unlike traditional grid-based methods, the unstructured finite element approach implemented in this study allows for the precise representation of sharp physical discontinuities and density contrasts, such as the core-mantle boundary and the inner-core interface. To ensure the reliability of our findings, we provide a rigorous quantitative validation of the numerical framework. We achieve this by benchmarking our simulated travel times and ray paths against analytical solutions derived from isotropic homogeneous models. This validation step demonstrates the methodology's accuracy in capturing complex wave kinematics and density-driven interactions. Consequently, this study establishes a validated computational platform for testing next-generation Earth models and exploring the sensitivity of seismic waves to abrupt structural transitions.

2. Methodology

In this study, the investigation of seismic wave propagation through complex Earth structures is conducted using a numerical forward modeling approach. This approach consists of a ray-based forward operator that utilizes Dijkstra's shortest path algorithm (Dijkstra, 1959). In this graph-based method, the mesh nodes serve as graph vertices, and Dijkstra's algorithm identifies the least-time path, providing a robust and computationally efficient discrete approximation to the continuous Eikonal ray-tracing problem – an approach well suited to the study's emphasis on first-order kinematics and travel-time accuracy. The methodology adopted here allows for the simulation of seismic responses based on predefined Earth models, providing a controlled environment to analyze the influence of varying subsurface parameters on wave behavior. The process involves several key steps: initial geometric discretization of the Earth's interior, quality inspection of the predefined computational domain (mesh) through analyses of a valid metric, assignment of material properties to the mesh based on different regions, and subsequent simulation of seismic wave propagation using established physical principles.

PREM defines radial variations in the physical properties of the Earth, including density (ρ), P-, and S-wave velocity (V_p , V_s), across distinct depth intervals. These properties are represented by piecewise cubic polynomials to ensure smooth transitions across the Earth's inherent layered structure. The general form of this representation is expressed as:

$$f(r) = a_0 + a_1 r + a_2 r^2 + a_3 r^3 \quad (1)$$

where $f(r)$ denotes the parameter value (e.g., ρ, V_p, or V_s) at radius r. Also, a_0, a_1, a_2, and a_3 are coefficients specific to each depth interval (Dziewonski & Anderson, 1981).

The accuracy and stability of numerical simulations are profoundly influenced by the quality of the underlying computational mesh. Mesh quality serves as a quantitative measure of how well individual mesh elements (e.g., triangular cells in 2D models) approximate ideal geometric shapes, which in turn directly impacts the precision and reliability of the numerical solution. A widely adopted metric for evaluating the quality (η) of a triangular element is given by (Field, 2000):

$$\eta = \frac{4\sqrt{3}a}{l_1^2+l_2^2+l_3^2} \quad (2)$$

Here, η represents the dimensionless mesh quality parameter. a denotes the area of the triangular element, while l_1, l_2, and l_3 are the lengths of its three sides. This metric is normalized such that an equilateral triangle, considered the optimal shape for numerical stability, yields a quality value of η=1. Conversely, as a triangular element becomes highly distorted, thin, or elongated (i.e., degenerate), its quality value η approaches 0.

To map the PREM P- and S-wave velocities and density contrasts onto the 2D computational mesh, the radial distance of each mesh cell center from the origin, corresponding to Earth's center, is first determined. This step is essential because PREM defines velocities and densities as a

function of radius in a 1D model, and the 2D mesh requires these parameters to be assigned based on the equivalent radial position of each cell to maintain consistency with Earth's spherical structure. The coordinates of each cell center are used to compute this distance, enabling the alignment of mesh points with the radial velocity profiles of PREM. Subsequently, the velocity and density data, tabulated as a function of radius, are interpolated onto these radial distances to assign appropriate values to each cell, creating continuous velocity and density fields across the mesh. This interpolation employs a linear method to estimate velocities and densities between PREM data points, ensuring a smooth velocity distribution, suitable for seismic wave propagation simulations. The applied linear interpolation was conducted within each PREM layer between consecutive radial points where the original piecewise polynomial values were evaluated. The interpolation is performed to estimate the parameter value P (where $P \in \{V_p, V_s, \rho\}$) at the radial distance r_n, as follows:

$$P(r_n) = P_i + \frac{P_{i+1}-P_i}{r_{i+1}-r_i}(r_n - r_i) \quad (3)$$

Here, $P(r_n)$ denotes the interpolated velocity (either P- or S-wave) and density at the radial distance r_n, representing the distance from Earth's center to a mesh cell center. The velocities or densities P_i and P_{i+1} are the PREM-systematized values at consecutive radial points r_i and r_{i+1}, respectively. These values bound the interval containing r_n and ensure precise mapping of PREM model parameters onto the computational mesh. Also, by applying the above-mentioned equation to the density profile, we ensure that the mass distribution within the mesh is consistent with radial stratification of PREM.

In the case of both velocity data types, the seismic survey geometry is established by assuming source and receivers on the Earth's surface within a plausible circular domain discretized through Delaunay triangulation. A single seismic source is positioned at one node of the outer boundary, with receivers placed at alternate nodes along half the circumference to capture wave arrivals at varying angular distances. This setup, implemented using a travel-time modeling framework, facilitates the simulation of seismic wave propagation through the PREM-based velocity models. It enables the computation of ray paths and travel times for subsequent analysis of apparent velocity curves.

To simulate seismic wave propagation through the PREM-based velocity models, travel times t are computed by integrating the slowness (reciprocal of velocity, $\frac{1}{v(x)}$) along ray paths (Rüger & Hale, 2006). This process, essential for determining the time taken for P- and S-waves to travel from the source to receivers, relies on the velocity distribution within the 2D mesh. The simplest form of the travel time calculation, suitable for the methodology section, is expressed as the integral of slowness over the ray path Γ through the medium, capturing the fundamental relationship between velocity and travel time (White, 1989). With ds as the differential path length (in meters) along the ray, this can be expressed like:

$$t = \int_\Gamma \frac{1}{v(x)} ds \quad (4)$$

Also, the trajectories are determined by solving the ray-tracing equation derived from the Eikonal approximation (Lin et al., 2009):

$$\frac{d}{dt}\left(\frac{1}{v(x)} \frac{dx}{dt}\right) = \nabla\left(\frac{1}{v(x)}\right) \quad (5)$$

Here, the term $\frac{dx}{dt}$ corresponds to the ray direction, scaled by the slowness $\frac{1}{v(x)}$. To evaluate the influence of Earth's layered structure on seismic wave propagation, the PREM-based model, incorporating depth-dependent velocity variations, is compared with both an isotropic homogeneous Earth model and a linear gradient model. In this simplified homogenous model, the Earth's internal structure is assumed to lack layering, with uniform material properties characterized by constant P- and S-wave velocities across the entire domain. Conversely, the linear gradient model assumes a smooth, continuous increase in velocity from the surface to the center, providing a benchmark to distinguish between global trends and the local effects of sharp discontinuities. This comparison, facilitated by simulating ray paths and apparent velocity curves across all three configurations, highlights the effects of velocity heterogeneities and layer boundaries

on seismic wave behavior and validates the necessity of PREM's discrete layering for accurate geophysical modeling.

3. Results and discussion

Numerical forward modeling illuminates seismic wave propagation through Earth's heterogeneous interior, employing the PREM and contrasting it with simplified homogeneous and linear gradient velocity models. By simulating P-wave and S-wave ray paths, travel times, and apparent velocities, the profound influence of Earth's layered structure is revealed, highlighting the critical role of velocity discontinuities in shaping wave behavior. Comparative analyses with idealized models, supported by precise geometric and survey configurations, clarify the necessity of detailed velocity structures for accurate geophysical modeling. These findings, derived from simulations rooted in PREM's comprehensive framework, offer critical insights into Earth's internal dynamics, advancing the understanding of seismic wave interactions and their implications for global seismology.

A schematic representation of Earth's internal structure, as illustrated in Figure 1a, delineates the crust, mantle, liquid outer core, and solid inner core, establishing the structural framework for numerical simulations. The diagram emphasizes critical boundaries, such as the Moho, core-mantle interface, and inner-outer core transition, which govern seismic wave interactions due to abrupt velocity changes. This layered configuration, based on PREM's radial structure, provides essential context for modeling wave propagation dynamics. By capturing the major structural divisions, the schematic underscores the importance of accurate boundary definitions in simulating complex wave interactions, setting the stage for detailed analyses of velocity variations and their geophysical implications. Figure 1b illustrates the graphical workflow of this study.

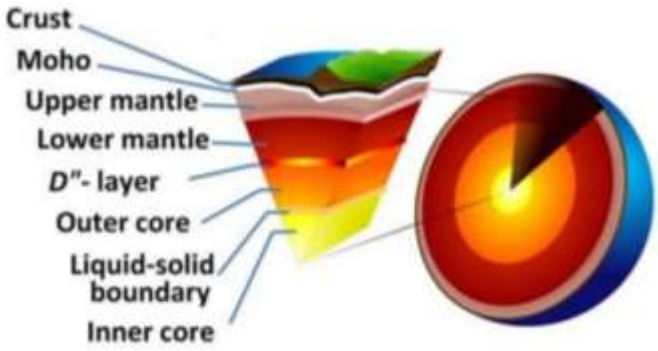

(a)

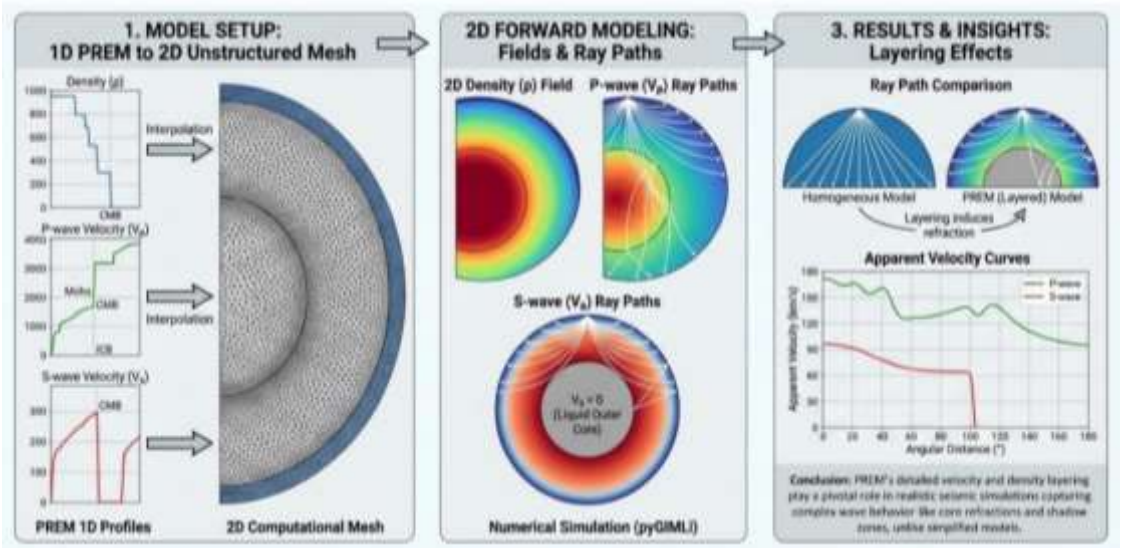

(b)

Figure 1. Schematic of the Earth's Internal Structure. (a) This diagram illustrates the main layers of the Earth: the crust, mantle, liquid outer core, and solid inner core. (b) Main implemented workflow in this study.

Radial variations in Earth's physical properties, derived from PREM and depicted in Figure 2, underpin the velocity models used in this study. Figure 2a reveals the density profile, characterized by gradual transitions within layers and sharp discontinuities at boundaries like the Moho and core-mantle interface, which significantly influence wave speeds. Figure 2b showcases P-wave (V_p) and S-wave (V_s) velocities, with pronounced radial variations and the absence of S-wave propagation in the liquid outer core – a hallmark of PREM's physical constraints. These profiles inform the computational framework, enabling precise simulation of seismic wave behavior across Earth's layered structure. The density and velocity variations highlight PREM's ability to capture Earth's complex internal architecture, a factor critical for accurate modeling of wave propagation and its application to seismic tomography. An open-source library named rockhound has been utilized to load the PREM data (Uieda & Soler, 2019).

The computational framework, implemented using the pyGIMLi library (version 1.4.3) (Rücker et al., 2017) on a laptop with 16 GB RAM and a 12th Gen Intel® Core™ i7-1255U CPU, relies on a geometric model and mesh, with parameters quantified in Table 1 and visualized in Figure 3. Concentric boundaries at the Earth's surface (6,371 km), outer core (3,490 km), and inner core (1,216 km) mirror PREM's structural divisions in Figure 3a, discretized with 48 segments for the Earth's surface and 32 segments for each core boundary to balance geometric accuracy with computational efficiency. Figure 3b displays a 2D unstructured mesh with a maximum element area of 10^{10} m², optimized to balance numerical accuracy with computational feasibility on the specified hardware. The mesh's predominantly equilateral triangular elements minimize numerical artifacts, facilitating robust velocity interpolation and reliable simulation of wave propagation across Earth's layered structure.

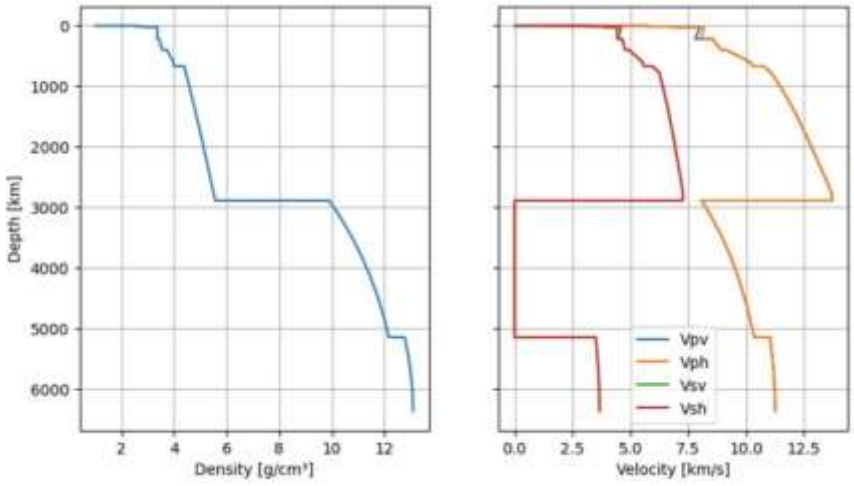

(a) (b)

Figure 2. Preliminary Reference Earth Model (PREM) Profiles. (a) Density and (b) P- and S-wave seismic velocities as a function of depth for PREM.

Table. 1 Geometric Model and Mesh Parameters for the 2D Earth Simulation.

Component	Parameter	Value
Earth's Surface	Radius	6,371 km
Outer Core Boundary	Radius	3,490 km
Inner Core Boundary	Radius	1,216 km
Earth Circle	Number of Segments	48
Outer Core Circle	Number of Segments	32
Inner Core Circle	Number of Segments	32
Mesh	Maximum Element Area	10^{10} m^2
Mesh	Boundary Count	31539
Mesh	Node Count	10631
Mesh	Element (Cell) Count	20909

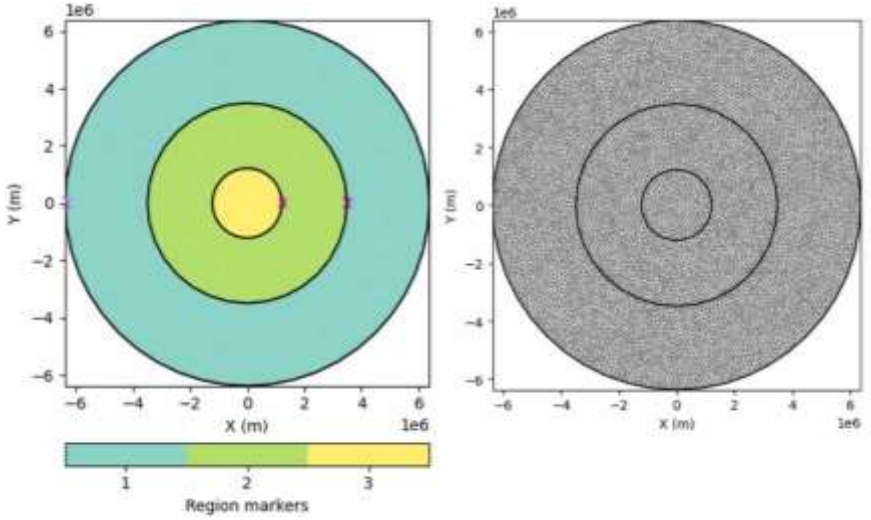

(a) (b)

Figure 3. Geometric Model and Computational Mesh of the Earth. (a) Initial geometric representation of the Earth's layered structure. (b) 2D unstructured mesh generated from the geometric model.

Numerical stability in simulations hinges on mesh quality, assessed through visualizations in Figure 4. A color scale in Figure 4a indicates element quality, ranging from 0 (severely distorted triangles) to 1 (equilateral triangles), while Figure 4b provides a histogram of quality metrics, confirming a high-quality mesh ($\eta \approx 1$). High mesh quality ensures precise ray-tracing and travel-time calculations, critical for capturing the effects of velocity discontinuities without introducing numerical errors. This stability is essential for modeling complex wave interactions in PREM-based simulations, particularly at boundaries like the core-mantle interface, where abrupt velocity changes drive significant refraction and reflection, impacting the accuracy of geophysical interpretations.

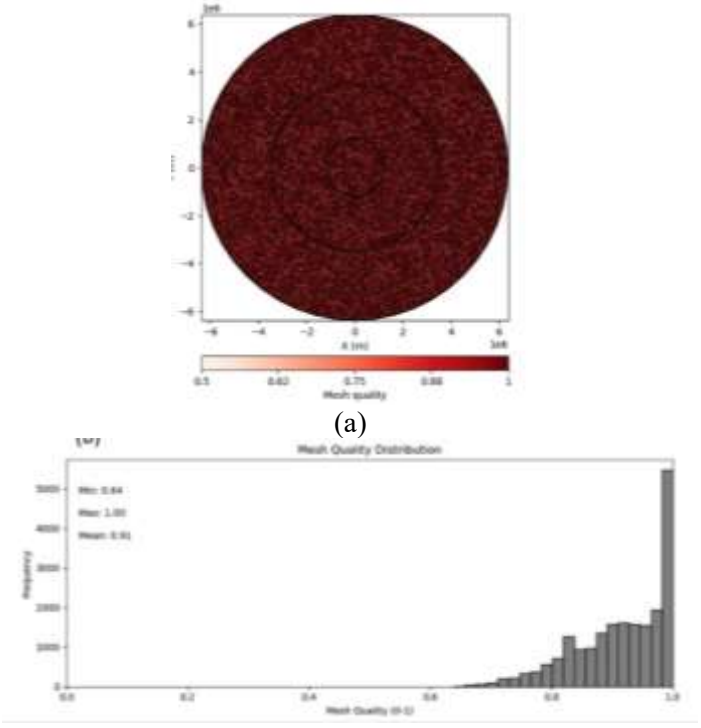

(a)

(b)

Figure 4. (a) Visualization of the mesh with individual cell quality indicated by color. Quality values range from 0 (poor) to 1 (perfect), with higher values indicating more equilateral triangles. (b) Histogram showing the distribution of mesh quality values across all cells. Insets display the minimum, maximum, and mean quality values for the mesh.

Velocity models and associated physical properties interpolated from PREM, as shown in Figure 5, form the cornerstone of the wave propagation simulations. Figure 5a shows the P-wave velocity (V_p) distribution, capturing transitions at boundaries like the Moho, transition zone, and core-mantle interface, reflecting Earth's heterogeneous structure. Figure 5b displays the S-wave velocity (V_s) distribution, with zero velocity in the liquid outer core, adhering to PREM's constraints. Figure 5c presents the interpolated density distribution, which provides the structural context for the velocity models and confirms the high-fidelity mapping of PREM's radial properties onto the 2D unstructured mesh. These models, mapped onto the 2D mesh, enable accurate computation of ray paths and travel times, critical for understanding how velocity heterogeneities influence wave propagation. The precise interpolation ensures that the models reflect Earth's layered architecture, providing a robust basis for geophysical analysis and applications in seismic inversion studies.

The simulation setup, configured by the seismic survey geometry detailed in Table 2 and illustrated in Figure 6, employs a single source at a surface node and receivers at alternate nodes along half the Earth's circumference (0° to 180°), with five secondary nodes per ray path to ensure smooth and accurate ray-tracing. This arrangement, embedded in a travel-time modeling framework, captures wave arrivals across diverse offsets, facilitating detailed computation of ray paths and travel times. The design ensures realistic conditions for studying the impact of Earth's internal structure on wave propagation, enabling analysis of how velocity variations affect seismic responses. The survey configuration supports the generation of apparent velocity curves and ray paths, providing insights into the complex interplay of waves with Earth's layered structure.

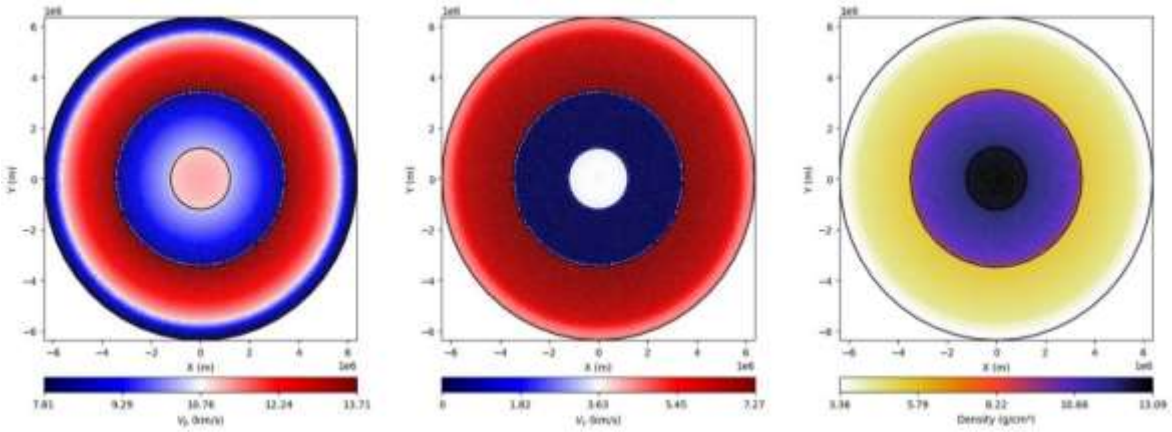

(a) (b) (c)

Figure 5. PREM P- and S-wave Velocity, and Density Models. (a) Interpolated V_p velocity model derived from PREM. (b) Interpolated V_s velocity model derived from PREM. (c) Interpolated ρ derived from PREM.

Table. 2. Seismic Survey Configuration for Wave Propagation Simulations.

Parameter	Value
Source Position	Node 0 (Earth's surface)
Number of Receivers	Half of total surface nodes
Receiver Distribution	Alternate nodes along half circumference
Angular Coverage	0° to 180°
Secondary Nodes per Ray Path	5

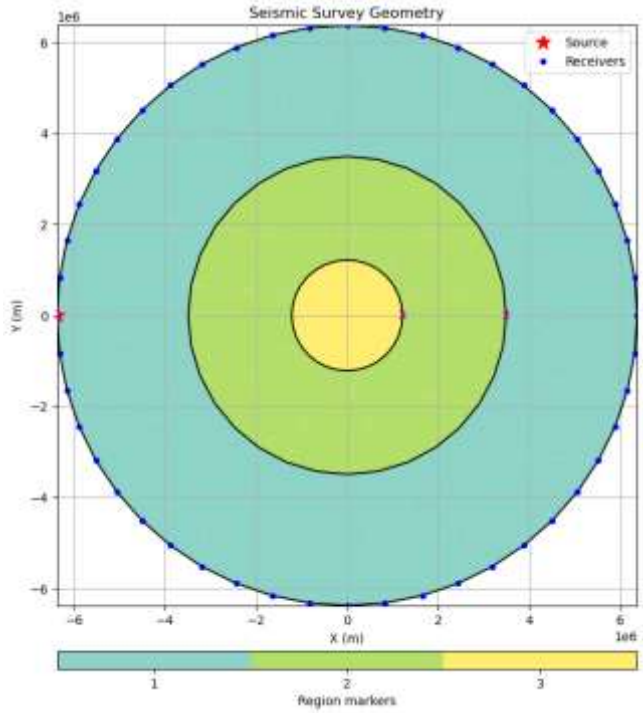

Figure 6. Seismic Survey Geometry on the Earth Model. This figure shows the placement of the seismic source (red star) and receivers (blue circles) along the Earth's surface for the forward modeling simulations.

Apparent velocity curves, derived from PREM-based models and plotted in Figure 7, compare P-wave and S-wave velocities as functions of angular distance. P-wave velocities consistently surpass S-wave velocities, reflecting their distinct propagation characteristics in Earth's heterogeneous interior. Quantitatively, P-wave apparent velocities range from 7.98 km/s to 12.06 km/s, while S-wave velocities vary from 4.57 km/s to 6.54 km/s. The curves exhibit pronounced variations corresponding to major discontinuities, such as the core-mantle boundary, where velocity gradients induce significant changes in wave speed. These findings highlight PREM's sensitivity to velocity heterogeneities, offering superior accuracy compared to simplified models with uniform or gradually varying velocities. The observed variations provide valuable data for seismic tomography, enabling refined models of Earth's internal structure and dynamics.

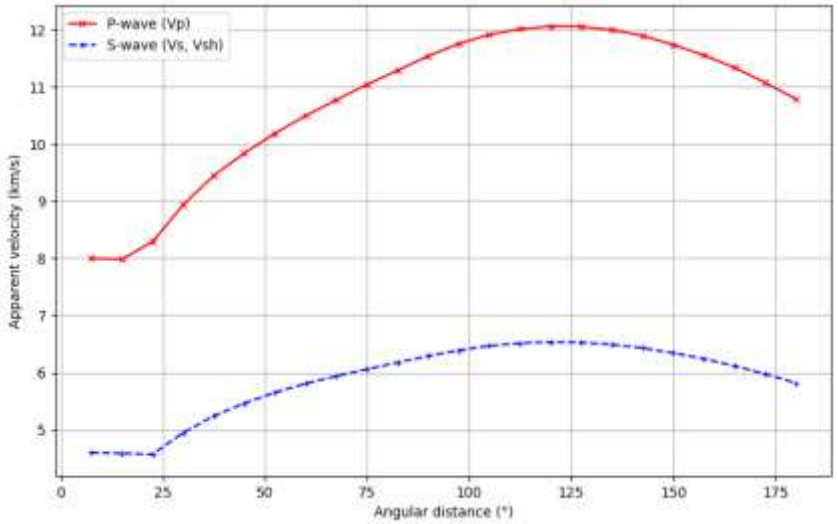

Figure 7. Apparent Velocity Curves for P-waves and S-waves from PREM. This plot compares the calculated apparent velocities for P-waves and S-waves as a function of angular distance from the source.

Ray paths through PREM velocity models, visualized in Figure 8, reveal intricate wave propagation trajectories. Figure 8a shows curved P-wave paths refracting at layer boundaries due to velocity gradients, reflecting the complex structure of Earth's interior. Figure 8b indicates no S-wave paths in the liquid outer core, consistent with PREM's zero S-wave velocity – a critical feature for accurate modeling. The trajectories, from source to receivers, demonstrate significant refraction and reflection at interfaces like the core-mantle boundary, underscoring PREM's ability to capture complex wave dynamics. These results highlight the importance of layered velocity models in simulating realistic seismic responses, with implications for understanding deep Earth processes.

In contrast, a homogeneous velocity model with a constant 10 km/s velocity, as depicted in Figure 9, produces linear ray paths. The absence of velocity gradients eliminates refraction effects, contrasting sharply with the curved paths observed in Figure 8. This simplicity fails to replicate the complex wave behavior induced by Earth's layered structure, highlighting the critical role of velocity heterogeneities. The homogeneous model's inability to capture refraction and reflection underscores the necessity of PREM for realistic seismic simulations, particularly for applications requiring accurate representation of deep Earth dynamics, such as mantle convection studies. To validate this framework, simulations on the homogeneous model were compared against analytical chord-distance travel times, yielding a mean relative error of only 0.2950% and a maximum error of 0.3985%.

Linear gradient velocity models, illustrated in Figure 10, assume smooth velocity decreases from the Earth's center (14 km/s for P-waves, 7 km/s for S-waves) to the surface (8 km/s for P-waves, 4 km/s for S-waves). Figure 10a shows the P-wave model, and Figure 10b the S-wave model, which inaccurately assigns non-zero S-wave velocity in the outer core – a significant limitation compared to PREM. These gradual transitions introduce refraction but oversimplify Earth's complex structure, failing to capture sharp discontinuities like the core-mantle boundary. The models provide a benchmark for evaluating continuous versus discontinuous velocity effects, revealing the importance of PREM's detailed layering for accurate seismic modeling.

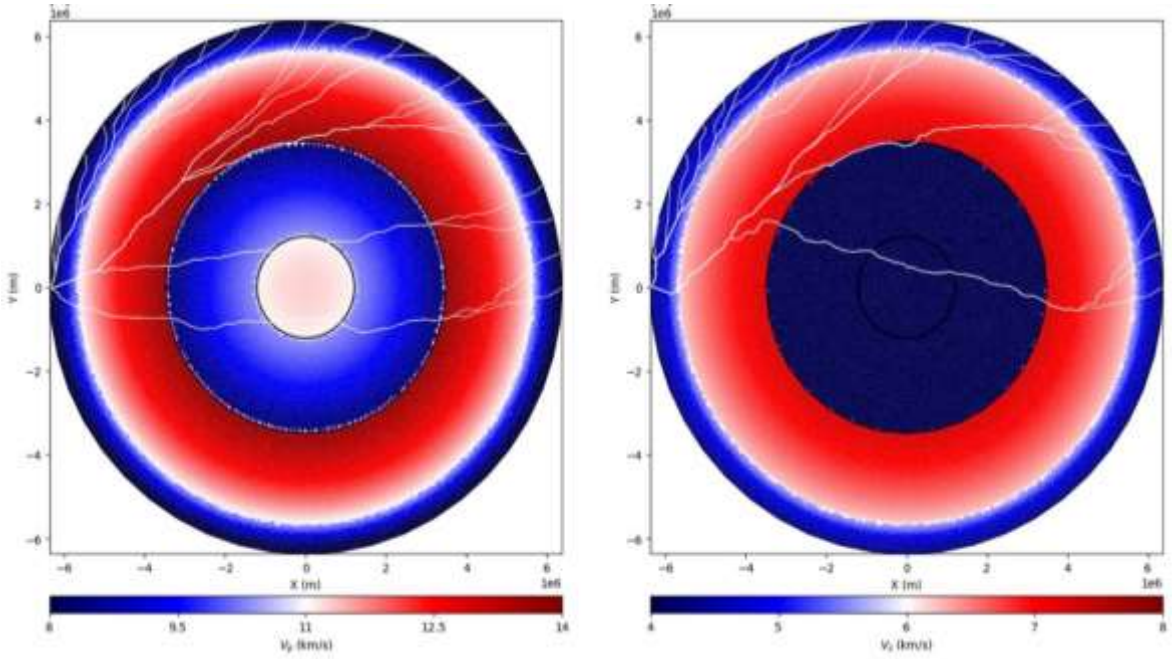

(a) (b)

Figure 8. Modeled Seismic Ray Paths through PREM Velocity Models. (a) P-wave velocity model (V_p) with corresponding ray paths. (b) S-wave velocity model (V_s) with corresponding ray paths. White lines denote the ray trajectories from the source to the receivers.

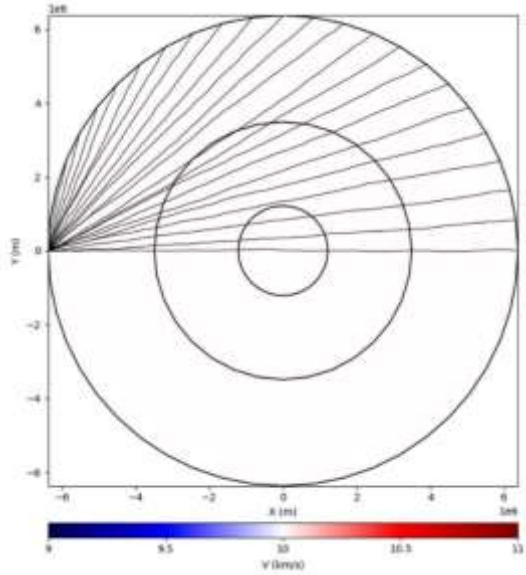

Figure 9. Homogeneous Velocity Model with Seismic Ray Paths. This plot displays a constant velocity model (10 km/s) across the entire Earth's cross-section, with overlaid ray paths shown as straight white lines.

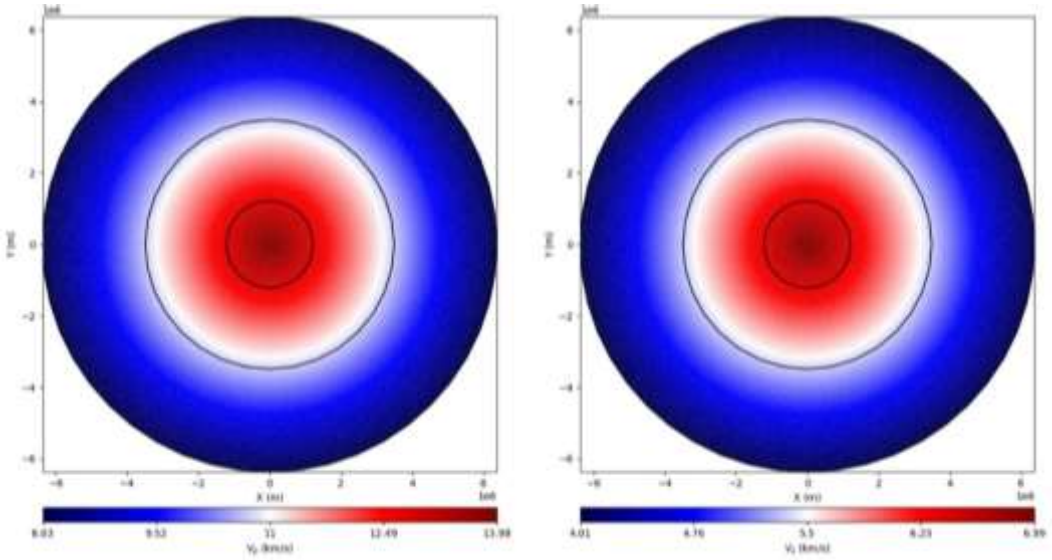

(a) (b)

Figure 10. Linear Gradient Velocity Models for P-waves (a) and S-waves (b). Both models show a smooth decrease in velocity from the Earth's center to its surface, displayed with a consistent color scale.

Comparative analysis of apparent velocity curves, shown in Figure 11, contrasts PREM with linear gradient models. Figure 11a indicates that PREM's P-wave velocities exhibit distinct variations due to layer boundaries, unlike the gradient model's smoother trends, which lack sharp transitions. At a 90° angular distance, the PREM P-wave travel time is approximately 24.22% faster than that of the linear gradient model, highlighting the influence of the high-velocity lower mantle – a feature not captured by the linear assumption. Figure 11b reveals significant S-wave deviations in PREM due to zero velocity in the outer core – a feature not present in the gradient model's continuous profile. These results validate PREM's capacity to produce realistic seismic responses, a capability critical for geophysical studies such as seismic tomography. The gradient model's oversimplification highlights the limitations of simplified velocity structures, reinforcing the importance of accurate discontinuities in modeling Earth's internal structural dynamics.

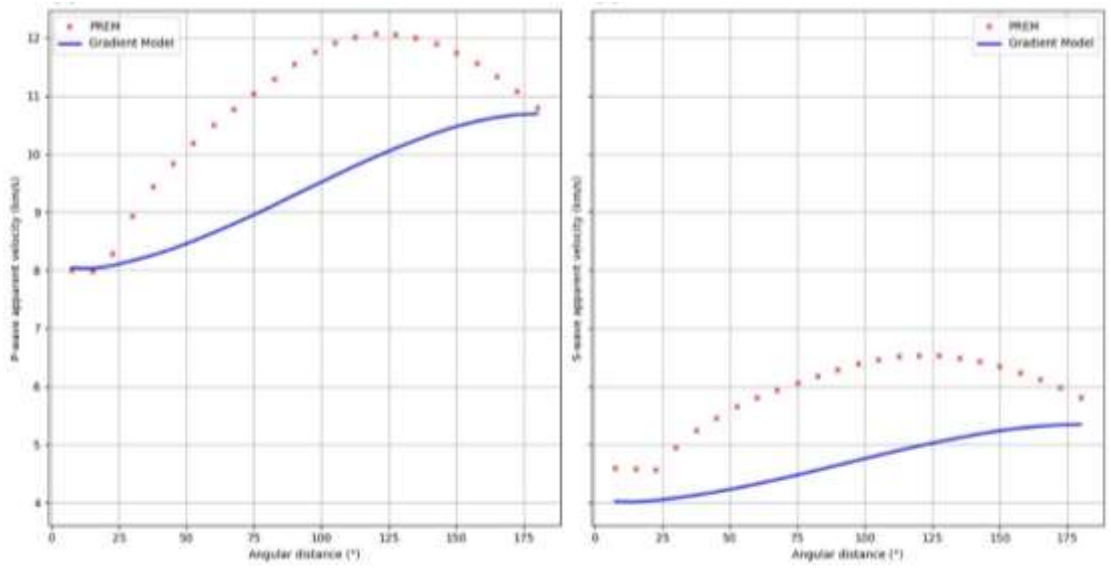

(a) (b)

Figure 11. Comparison of Apparent Velocity Curves from PREM and Linear Gradient Models. (a) P-wave apparent velocity. (b) S-wave apparent velocity.

To scrutinize the transition zones, 1D velocity profiles were extracted radially from the center to the surface (Figure 12). Unlike the continuous slopes of the gradient model, the PREM extraction accurately captures the velocity jump at the Core-Mantle Boundary (CMB) and the subtle transitions within the upper mantle. This 1D comparison confirms that the numerical interpolation onto the 2D triangular mesh preserves the fundamental physical discontinuities of the original 1D PREM equations, ensuring that subsequent ray-tracing accounts for the sharp refraction interfaces required for global seismic tomography.

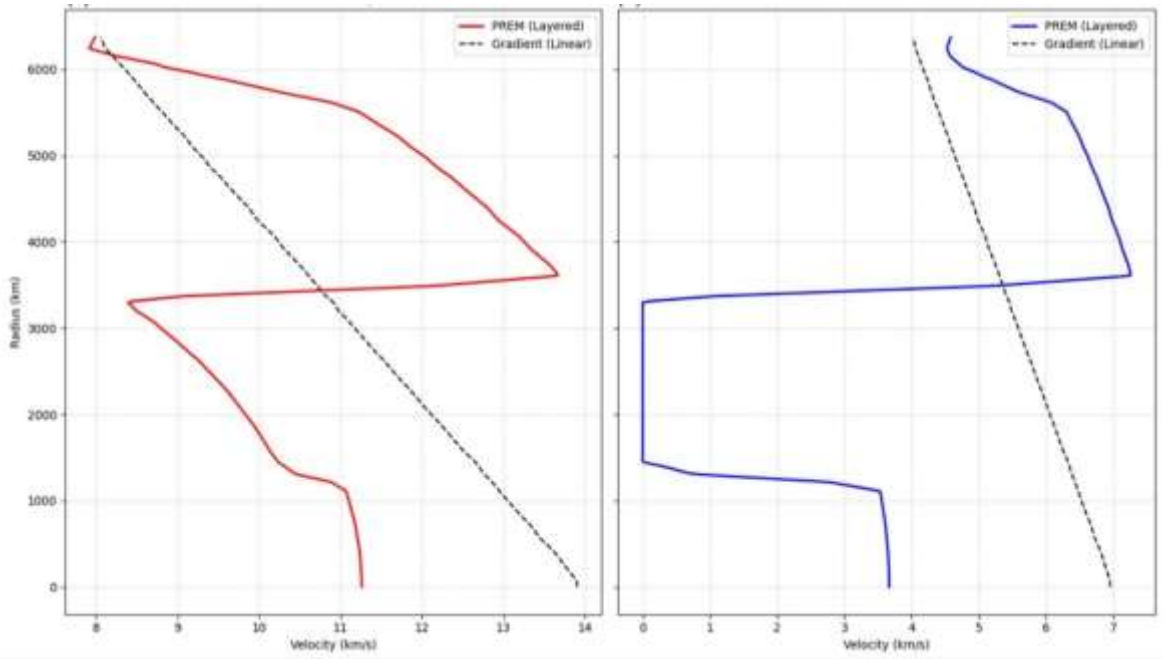

(a) (b)

Figure 12. Radial velocity profiles extracted from 2D numerical models**.** (a) P-wave velocity (V_p) and (b) S-wave velocity (V_s) comparison between the layered PREM (solid lines) and the linear gradient model (dashed lines). The 1D profiles, extracted radially from the center (r = 0) to the surface (r = 6,371 km), highlight the sharp velocity discontinuities at the core-mantle boundary and the S-wave shadow zone in the liquid outer core, features that are simplified by the continuous gradient approach.

The relative deviation between the linear gradient and PREM models, mapped as a spatial perturbation, reveals the structural limitations of simplified models (Figure 13). The gradient model shows a maximum underestimation of velocity by -22.93% in the lower mantle, while overestimating core velocities significantly – up to 31.68%. This "relativity plot" provides a visual diagnostic of where smooth gradient assumptions fail, reinforcing the necessity of layered reference models like PREM for identifying deep-Earth anomalies and mantle convection patterns. Furthermore, Table 3 encompasses some details about the travel times explicitly.

4. Conclusion

The numerical forward modeling conducted in this study elucidates the critical influence of Earth's layered structure on seismic wave propagation by implementing the Preliminary Reference Earth Model (PREM) within a 2D computational framework. Through the systematic simulation of P-wave and S-wave ray paths, travel times, and apparent velocity curves, the distinct seismic responses generated by PREM's velocity heterogeneities and layer boundaries are clearly demonstrated. Validation against analytical homogeneous solutions yielded a very low mean travel-time error, confirming the precision of the discretized geometry.

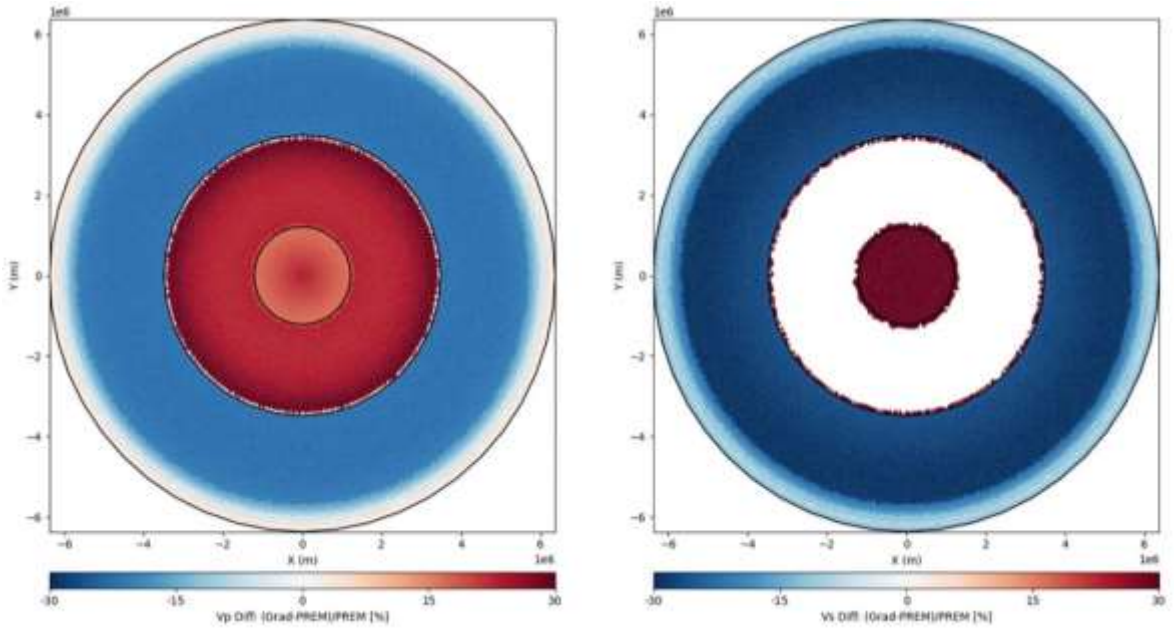

(a) (b)

Figure 13. Relative velocity perturbation maps between the linear gradient and PREM models. (a) P- and (b) S-wave relative differences. Red regions indicate where the gradient model overestimates velocity (primarily in the lower mantle), while blue regions indicate underestimation. The S-wave map (b) highlights the fundamental discrepancy in the outer core region where the gradient model erroneously assumes shear stiffness.

Table. 3. Quantitative comparison of P-wave travel times. Numerical results for PREM and linear gradient models at key angular distances, including the relative percentage difference

Angle (°)	PREM (s)	Gradient (s)	Difference (%)
30	369.00	403.94	9.74
60	606.91	736.96	21.43
90	780.53	969.55	24.22
120	914.73	1109.01	21.24
150	1048.36	1175.16	12.09
180	1180.62	1191.78	0.94

Comparisons with simplified homogeneous and linear gradient velocity models reveal that the absence of layering or sharp discontinuities – as in the homogeneous model – results in overly simplistic wave behavior with straight ray paths, while the gradient model, despite introducing continuous velocity variations, fails to capture the complex refractions observed in PREM, particularly in regions like the liquid outer core where S-wave propagation is absent. These findings underscore the superiority of PREM in accurately representing Earth's internal dynamics for seismic studies.

We acknowledge the assumption of spherical symmetry as a limitation; however, this framework establishes a baseline for future simulations. The high-quality computational mesh and precise interpolation of PREM velocities ensure robust and reliable simulations, highlighting the effectiveness of advanced numerical techniques, such as finite element methods and unstructured meshing, in modeling complex geophysical systems. This study reaffirms the enduring relevance of PREM as a cornerstone for seismic modeling while emphasizing the need for detailed velocity models to achieve realistic simulations of wave propagation. Future work could extend these analyses by incorporating three-dimensional models or advanced inversion techniques to further refine our understanding of Earth's interior and validate next-generation reference models against emerging seismic datasets.

Acknowledgements

We would like to express our sincere thanks to the School of Mining Engineering at the University of Tehran for providing an excellent academic environment and the resources necessary to complete this research.

Availability of data and materials

The datasets generated and/or analyzed during the current study, and the python script are available at Github with the following link: https://github.com/AY131313/PREM-2025

References

Ammon, C. J., Velasco, A. A., Lay, T., & Wallace, T. C. (2021). Earth structure. In *Foundations of Modern Global Seismology* (pp. 269–301). Elsevier. https://doi.org/10.1016/B978-0-12-815679-7.00017-3

Bormann, P., Robert Engdahl, E., & Kind, R. (n.d.). *Chapter 2 Seismic Wave Propagation and Earth models*. https://doi.org/10.2312/GFZ.NMSOP-2_ch2

Cammarano, F., Deuss, A., Goes, S., & Giardini, D. (2005). One-dimensional physical reference models for the upper mantle and transition zone: Combining seismic and mineral physics constraints. *Journal of Geophysical Research: Solid Earth*, *110*(B1). https://doi.org/10.1029/2004JB003272

De Basabe, J. D., & Sen, M. K. (2009). New developments in the finite-element method for seismic modeling. *The Leading Edge*, *28*(5), 562–567. https://doi.org/10.1190/1.3124931

Dijkstra, E. W. (1959). A note on two problems in connexion with graphs. *Numerische Mathematik*, *1*(1), 269–271. https://doi.org/10.1007/BF01386390

Dziewonski, A. M., & Anderson, D. L. (1981). Preliminary reference Earth model. *Physics of the Earth and Planetary Interiors*, *25*(4), 297–356. https://doi.org/10.1016/0031-9201(81)90046-7

Field, D. A. (2000). Qualitative measures for initial meshes. *International Journal for Numerical Methods in Engineering*, *47*(4), 887–906. https://doi.org/10.1002/(SICI)1097-0207(20000210)47:4<887::AID-NME804>3.0.CO;2-H

Guliyev, H. H., & Javanshir, R. J. (2020). Once Again on Preliminary Reference Earth Model. *Earth and Space Science*, *7*(3). https://doi.org/10.1029/2019EA001007

Lin, F.-C., Ritzwoller, M. H., & Snieder, R. (2009). Eikonal tomography: surface wave tomography by phase front tracking across a regional broad-band seismic array. *Geophysical Journal International*, *177*(3), 1091–1110. https://doi.org/10.1111/j.1365-246X.2009.04105.x

Ma, X., & Tkalčić, H. (2021). CCREM: New Reference Earth Model From the Global Coda-Correlation Wavefield. *Journal of*

Geophysical Research: Solid Earth, *126*(9). https://doi.org/10.1029/2021JB022515

Montagner, J.-P., & Kennett, B. L. N. (1996). How to reconcile body-wave and normal-mode reference earth models. *Geophysical Journal International*, *125*(1), 229–248. https://doi.org/10.1111/j.1365-246X.1996.tb06548.x

Morelli, A., & Dziewonski, A. M. (1993). Body Wave Traveltimes and A Spherically Symmetric P- and S-Wave Velocity Model. *Geophysical Journal International*, *112*(2), 178–194. https://doi.org/10.1111/j.1365-246X.1993.tb01448.x

Peter, D., Komatitsch, D., Luo, Y., Martin, R., Le Goff, N., Casarotti, E., Le Loher, P., Magnoni, F., Liu, Q., Blitz, C., Nissen-Meyer, T., Basini, P., & Tromp, J. (2011). Forward and adjoint simulations of seismic wave propagation on fully unstructured hexahedral meshes. *Geophysical Journal International*, *186*(2), 721–739. https://doi.org/10.1111/j.1365-246X.2011.05044.x

Rettenberger, S., & Bader, M. (2015). Optimizing I/O for Petascale Seismic Simulations on Unstructured Meshes. *2015 IEEE International Conference on Cluster Computing*, 314–317. https://doi.org/10.1109/CLUSTER.2015.51

Rücker, C., Günther, T., & Wagner, F. M. (2017). pyGIMLi: An open-source library for modelling and inversion in geophysics. *Computers and Geosciences*, *109*, 106–123. https://doi.org/10.1016/j.cageo.2017.07.011

Rüger, A., & Hale, D. (2006). Meshing for velocity modeling and ray tracing in complex velocity fields. *GEOPHYSICS*, *71*(1), U1–U11. https://doi.org/10.1190/1.2159061

Shearer. P. (2009). The PREM model. In *Introduction to Seismology* (pp. 349–352). Cambridge University Press. https://doi.org/10.1017/CBO9780511841552.014

Song, X., & Helmberger, D. V. (1995). A *P* wave velocity model of Earth's core. *Journal of Geophysical Research: Solid Earth*, *100*(B6), 9817–9830. https://doi.org/10.1029/94JB03135

Tenzer, R., Ji, Y., & Chen, W. (2022). The Accuracy Assessment of the PREM and AK135-F Radial Density Models. *Sensors*, *22*(11), 4180. https://doi.org/10.3390/s22114180

Uieda, L., and Soler, S.R. (2019). Rockhound: Download geophysical models/datasets and load them in Python (Version 0.1.0). Zenodo. https://doi.org/10.5281/zenodo.3086002

Wang, H., Xiang, L., Jia, L., Jiang, L., Wang, Z., Hu, B., & Gao, P. (2012). Load Love numbers and Green's functions for elastic Earth models PREM, iasp91, ak135, and modified models with refined crustal structure from Crust 2.0. *Computers & Geosciences*, *49*, 190–199. https://doi.org/10.1016/j.cageo.2012.06.022

White, D. J. (1989). Two-Dimensional Seismic Refraction Tomography. *Geophysical Journal International*, *97*(2), 223–245. https://doi.org/10.1111/j.1365-246X.1989.tb00498.x

Zeng, L., Sasselov, D. D., & Jacobsen, S. B. (2016). MASS–RADIUS RELATION FOR ROCKY PLANETS BASED ON PREM. *The Astrophysical Journal*, *819*(2), 127. https://doi.org/10.3847/0004-637X/819/2/127